

Estimation of geothermal well discharges with artificial neural networks

Dr. İsmail KILINÇ,

Phd of Civil Engineering

ismail_kilinc@yahoo.com

Keywords: geothermal well production, radial basis functions, artificial neural networks, prediction

ABSTRACT

Geothermal power generation is increasingly important. The electricity generation of the geothermal power plant depends on many factors such as the discharge and the temperature of the geothermal fluid coming from the production well and the outdoor temperature in the environment where the plant is located. From these factors, only fluid discharge will be considered in this study. The effect of underground dynamics, pressure variation, gas concentration, and the performance of other wells fed from the same reservoir affect the production of a production well on an hourly basis. This directly affects the amount of gross production in that time zone, as well as the amount of re-injection pump power change, cooling tower energy consumption and similar processes as an amount of domestic consumption by the incoming fluid flow.

For this reason, the prediction of the well fluid discharge is very important in terms of production and consumption planning.

Artificial neural networks are predictive and modelling tools used in many areas of science. In engineering, there are often many application areas in the completion of missing data. Artificial neural networks, like other artificial intelligence models, are based on algorithms learned from the available data. In this study, artificial neural network method based on Radial based functions was used.

The daily production quantities for the next 7-day processes were tried to be estimated using Radial basis functions and compared with actual values using a 155-day production data of a real-time production well of a real plant in this study. The study considers that production planning and forecasting of energy sales contracts for the future are important from an estimation point of view.

1. INTRODUCTION

1.1 Geothermal Energy in Turkey

Turkey is located between different tectonic zones on the Alpine-Himalayan orogenic belt. As a result Turkey has a very wide potential of geothermal energy. Geothermal energy in Turkey is mainly used for direct applications of heating, aquaculture, and industrial processes and to generate electricity. (Bilgin, O. 2018)

According to the information from the Ministry of Energy, in the case of the geothermal capacity; Turkey is one of the top five countries in this area together with USA, Philippines, Indonesia and New Zealand.

The geothermal areas in the country are mainly located in western part. Such as 78% of the geothermal fields are situated in Western Anatolia, 9% in Central Anatolia, 7% in the Marmara Region, 5% in Eastern Anatolia and 1% in the other regions.

90% of Turkey's geothermal resources are low and medium enthalpy geothermal areas which are suitable for direct applications (heating, thermal tourism, industrial usage, etc.), while remaining 10% are suitable electricity generation. For the direct use purposes, 55% of the geothermal areas in Turkey are suitable for heating applications. Geothermal energy is employed to heat 1200 decares of greenhouse and 100,000 houses in 15 settlements are heated with geothermal energy (Demirbas, A., 2002). Balikesir-Gonen, Kutahya-Simav, Kirsehir, Kizilcahamam, Izmir-Balcova, Afyon-Omer, Izmir-Narlidere, Afyon-Sandikli, Kozakli ve Diyardin fields are spotted for heating purposes (Demirbas, A., 2002)

Total direct use of geothermal energy in the world with same reference is higher than 70.000 MWt as of year 2018. Top 5 countries in direct usage applications are USA, China, Sweden, Belarus and Norway. (Ministry of Energy, 2018)

The installed capacity of geothermal energy as of year 2018 was 14.369 GWe in Turkey. Since 2005, with the support of our Ministry, the development of existing geothermal resources initiated and began to search for new potential areas. As the end of 2004, the available heat capacity of 3.100 MWt increased to 5.000 MWt by an additional 1.900 MWt heat energy.

173 discovered geothermal fields reached to 239 fields which 10 of them are suitable for electricity production. So far, total of 632 drillings with total of 410.000 meters of depth and approximately 5.000 MWt of heat energy (including natural springs) obtained from these wells. (Demirbas, A., 2002)

In 2008, in conjunction with the Geothermal Resources and Natural Mineralized Waters Law, private sector began to introduce development and investment of geothermal projects also. In conjunction with this development, the country's total geothermal heat capacity (visible amount of heat) reached to 35.500 MWt. (Demirbas, A., 2002)

Turkey's geothermal potential is concentrated in Western Anatolia (77.9%) but only 13% of this potential (approximately 4000 MW) was made available for use by MRE (Mineral Research and Exploration Institute). (Demirbas, A., 2002) Turkey has a rich geothermal energy potential due to the influence of different tectonic belts originating from Alpine-Himalayan Orogenesis and a part of this potential is used in diverse applications. The most important fields for electricity generation and their fluid temperature values are presented below in Figure 1. (Bilgin, O. 2018)

These fields can be listed as Aydın-Germencik (232°C), Aydın-Buharkent (127°C), Denizli-Kizildere (242°C), Denizli-Nazilli (127°C), Canakkale-Tuzla (173°C), Aydın-Salavatlı (171°C) Manisa-Salihli-Caferbeyli (155°C), Manisa-Alaşehir (287.5) Kutahya-Simav (162°C), Kutahya-Şaphane (181°C), İzmir-Seferihisar (153°C), İzmir-Dikili (130°C), İzmir-Balçova (136°C).



Figure 1. Main powerplants generating electricity with geothermal resources in Turkey Aegean Region (Bilgin, O. 2018)

1.2 Geothermal power plants for electricity

Geothermal power plants are used in order to generate electricity by the use of geothermal energy. They essentially work the same as a coal or nuclear power plant, the main difference being the heat source.

Hot geothermal water or steam or both together is extracted from the Earth through a series of wells and feeds the power plant. In most of the geothermal plants the heat of the geothermal source is extracted to generate electricity. Then the water pulled up from the ground is returned back to the subsurface by re-injection wells. Donev et al. (2017).

There are 3 main types of geothermal power plants.

- 1- Dry steam plants
- 2- Binary cycle plants
- 3- Flash cycle steam plants

The type of plant depends on the available geothermal energy. The temperature and the discharge of each well is very important for the production rate and also type of the power plant.

Dry steam power plants use dry steam that is naturally produced by the earth. This steam travels from the production well to the surface and through a turbine, and after transferring its energy to the turbine it condenses and is injected back into the Earth. These types are the oldest types of geothermal power plants, the first one was built back in 1904 in Italy. Because this type of power plant requires the highest temperatures they can only be used where the temperature underground is quite high, but this type requires the least fluid flow. (Donev et al. 2017)

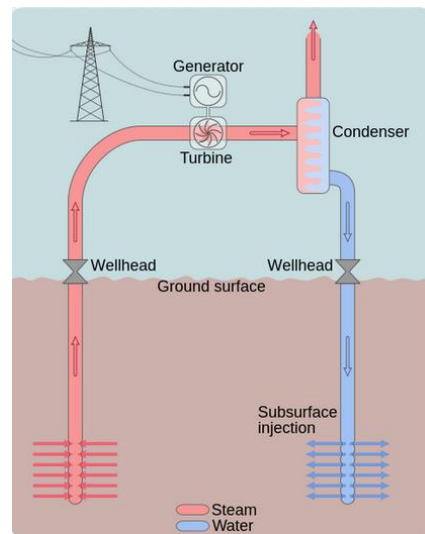


Figure 2. Dry steam cycle. (Donev et al. 2017)

Flash cycle steam plants are the most common due to the lack of naturally occurring high-quality steam. In this method, water under its own pressure it flows upwards through the well. This is a lower temperature than dry steam plants have. As its pressure decreases, some of the water "flashes" to steam, which is passed through the turbine section. The remaining water that did not become steam is cycled back down into the well and can also be used for heating purposes. The cost of these systems is increased due to more

complex parts, however they can still compete with conventional power sources.

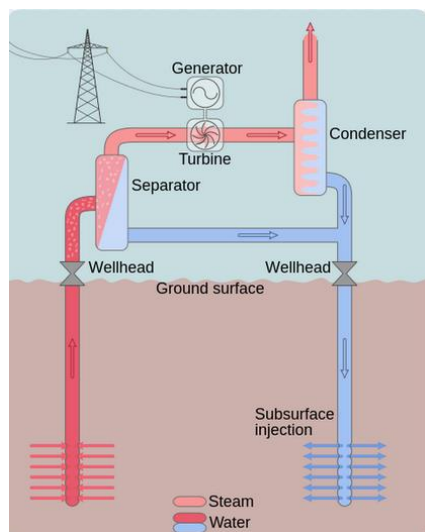


Figure 3. Flash steam cycle (Donev et al. 2017)

Binary power plants are expected to be the most commonly used type of geothermal power plant in the future, as locations outside of the known hot spots begin to use geothermal energy. This is because binary cycle plants can make use of lower temperature water than the other two types of plants. They use a secondary loop (hence the name "binary") which contains a fluid with a low boiling point, such as pentane or butane. The water from the well flows through a heat exchanger which transfers its heat to this fluid, which vaporizes due to its low boiling point. It is then passed through a turbine, accomplishing the same task as steam. (Donev et al. 2017)

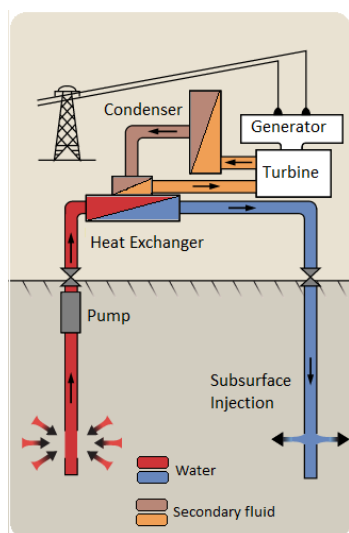


Figure 4. Binary cycle. The lighter brown is vaporized butane, while darker brown is liquid butane (Donev et al. 2017)

2. ARTIFICIAL NEURAL NETWORKS

Artificial Neural network tools are derived from the massively parallel biological structures found in human brain system. A neural network has an input layer, a hidden layer and an output layer. Each layer is

made up of several nodes, and layers are interconnected by sets of weights. The pattern of connectivity and the number of neurons in each layer may vary within some constraints. A very simple configuration of an ANN is presented as figure 5.

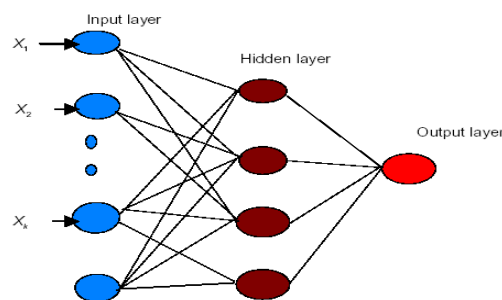


Figure 5: Basic configuration of an Artificial Neural Network

The application of the ANN to forecast and estimate the given data is composed of two steps by using some computer programs. The first step was the training of the neural networks. It is also called as the learning phase. The network "learns" by adjusting the interconnections (called weights) between layers. When the network is adequately trained, it is able to generalize relevant output for a set of input data. A valuable property of neural networks is that of generalization, whereby a trained neural network is able to provide a correct matching in the form of output data for a set of previously unseen input data. Learning typically occurs by example through training, where the training algorithm iteratively adjusts the connection weights (synapses) (Ajith et al,2001).

There are several different types of neural networks. In this study Radial Basis Functions (RBF). Radial Basis Functions networks were introduced into the neural network literature by Broomhead and Lowe in 1988. The RBF network model is motivated by the locally tuned response observed in biological neurons. Neurons with a locally tuned response characteristic can be found in several parts of the nervous system, for example, cells in the visual cortex sensitive to bars oriented in a certain direction or other visual features within a small region of the visual field (Poggio and Girosi 1990). These locally tuned neurons show response characteristics bounded to a small range of the input space

The theoretical basis of the RBF approach lies in the field of interpolation of multivariate functions. The objective of interpolating a set of tuples

$$(x^s, y^s)_{s=1}^N \text{ with } x^s \in R^d$$

is to find a function

$F : \mathbb{R}^d \rightarrow \mathbb{R}$ with $F(x_s) = y_s$ for all $s = 1, \dots, N$

where F is a function of a linear space.

In the RBF approach the interpolating function F is a linear combination of basis functions

$$F(x) = \sum_{s=1}^N w_s \phi(\|x - x^s\|) + p(x) \quad [1]$$

where $\|\cdot\|$ denotes Euclidean norm, w_1, \dots, w_N are real numbers, ϕ is a real valued function, and $p \in \prod_n^d$ a polynomial of degree at most n (fixed in advance) in d variables. The interpolation problem is to determine the real coefficients w_1, \dots, w_N and the polynomial term $p = \sum_{l=1}^D a_l p_l$ where p_1, \dots, p_D is the standard basis of \prod_n^d and a_1, \dots, a_D are real coefficients.

The solution of the exact interpolating RBF mapping passes through every data point (x_s, y_s) . In the presence of noise, the exact solution of the interpolation problem is typically a function oscillating between the given data points. An additional problem with the exact interpolation procedure is that the number of basis functions is equal to the number of data points and so calculating the inverse of the $N \times N$ matrix ϕ becomes intractable in practice. The interpretation of the RBF method as an artificial neural network consists of three layers: a layer of input neurons feeding the feature vectors into the network; a hidden layer of RBF neurons, calculating the outcome of the basis functions; and a layer of output neurons, calculating a linear combination of the basis functions. Different numbers of hidden layer neurons and spread constants are examined in the study. The hidden layer neurons' numbers that give the minimum mean square errors (MSE) are found to vary between 14 and 20. The spread is a constant which is selected before RBF simulation. The spreads that give the minimum MSE are between 0.03 and 6.3.

Artificial neural network models are widely used in different areas of life. They are mainly used for forecasting the time series such as financial data, hydrological data, meteorological data, medical and biological data etc.

3. CASE STUDY, DISCHARGE FORECAST OF PRODUCTION WELLS

This case study is mainly focussed on the hourly brine discharges of a geothermal power plant. The power plant is located in Aydın province of Turkey. Aydın province is the main geothermal area in Turkey. It is located in Menderes basin which is an important earthquake zone. Several power plants of different companies are in operation and generating an important amount of electricity that is produced from geothermal resources. The power plant in the scope of this study has an installed capacity of 24 MWs. It is a combination of two units of turbines each of 12 MW. It has been in operation for 3 years. There are 7 production wells and 6 re-injection wells for pumping the brine into the ground. The design discharge was 1940 m³/hours of brine in 145 degrees Centigrade. Due to several reasons the output of the production wells are being decreasing. So that the discharge is differing in hour timescale.

The aim of the study is to forecast the hourly mean total discharges of the production wells in daily basis. This is for the optimization of the operating plans of the power plant so that the maximum commercial benefit is being obtained.

Figure 6 is illustrated for information about the data used in this study. From the beginning of the year 2018 to June the hourly average discharge of each day is presented as a linear graph to visualize the real time condition.

It is obvious that there is a decrease. The decrease from the beginning is due to some reasons such as interaction of neighbouring power plants, seasonality or some other technical problems in the plant.

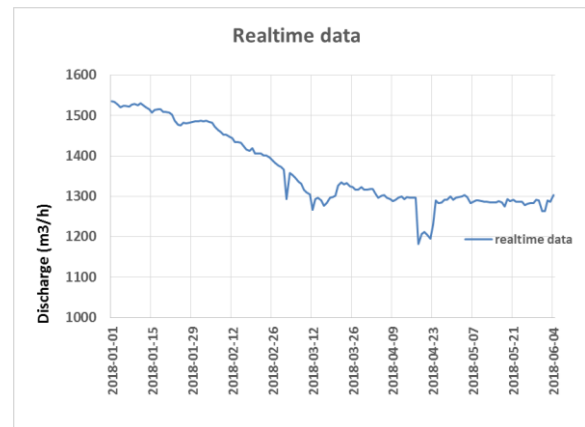


Figure 6. Hourly discharges of the production wells for 5 months.

Radial basis functions is a widely used kind of artificial neural networks. Time series problems are commonly simulated with radial basis functions. In this case study average hourly discharges for each day is used for forecasting the same values for the next week.

Table 1 is presenting the summary of all simulations performed with radial basis functions.

Table 1 shows that 3 main group of simulations with radial basis functions were performed. In the first row the input layer cells were the datum of previous 6 days of the target date. As the simplest definition the data from Monday to Saturday were taken into account for obtaining Sunday's data. In the second row the previous five days data were in the input layer cells. The spread parameter was found 0.54 in the optimum case. Number of neurons are 9. The third row of the table simply presents us that the five previous days were in charge to find tomorrow's data. That is why for example during a day time that we do not have that day's data but we want to estimate tomorrow's data.

In the first group of simulations a data set of 155 days is simulated with radial basis functions. In the input layer cells, the daily average of previous six days were used in the training phase of the neural networks. The spread parameter was taken 0.53 and the number of neurons were taken as 10. 148 days data was trained and then tested for the real time data of next 7 days.

The output layer cell was called as Q(t) was forecasted with a mean square error (MSE) of 14.06 with an R2 of 0.991. Here R2 refers as the determination coefficient that is commonly known as the square of correlation coefficient.

Figure 7 and Figure 8 represents the results of the simulations 6 previous days input layer cells.

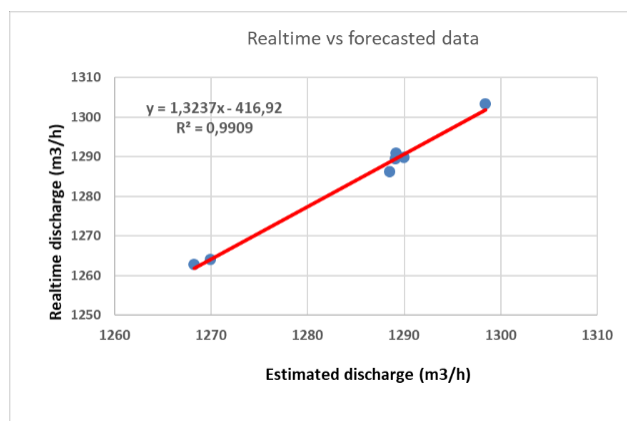


Figure 7. Correlation of observed data and forecasted data using 6 previous days datum input layer cells

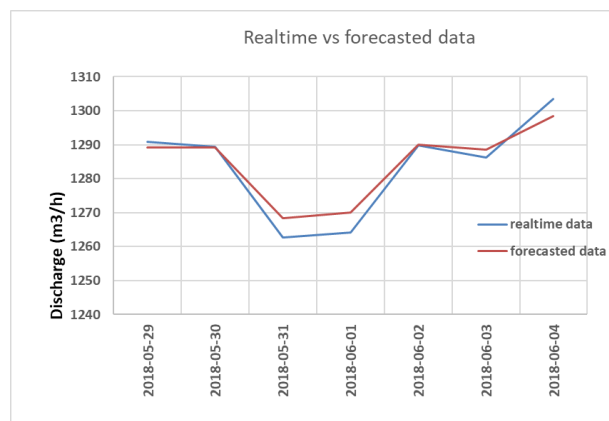


Figure 8. Observed data and forecasted data using 6 previous days datum input layer cells presented together

In the second group of simulations presented in the second row of the table 1, the same data set of 155 days is taken into account by the radial basis functions. In the input layer cells, the daily average of previous five days were used in the training phase of the neural networks. The spread parameter was taken 0.54 and the number of neurons were taken as 10. 148 days data was trained and then tested for the real time data of next 7 days.

The output layer cell was called as Q(t) was forecasted with a mean square error (MSE) of 19.89 with an R2 of 0.988. Here R2 refers as the determination coefficient that is commonly known as the square of correlation coefficient.

Figure 9 and Figure 10 represents the results of the simulations 5 previous days input layer cells.

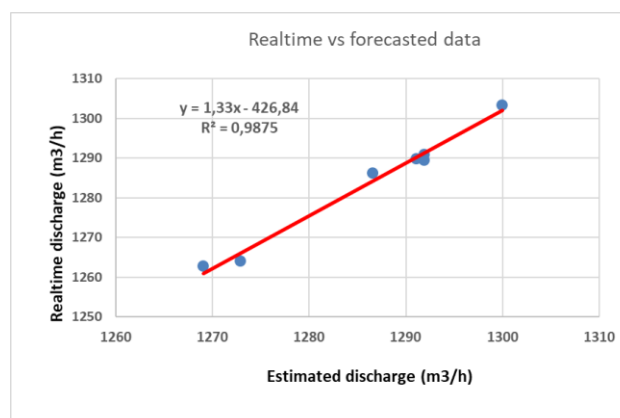


Figure 9. Correlation of observed data and forecasted data using 5 previous days datum input layer cells

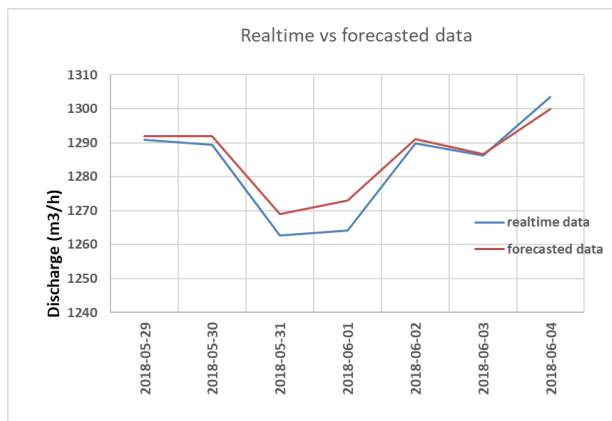


Figure 10. Observed data and forecasted data using 5 previous days datum input layer cells presented together

In the last group of simulations presented in the third row of the table 1, the same data set of 155 days is taken into account by the radial basis functions. In the input layer cells, the daily average of previous five days were used in the training phase of the neural networks. Its difference from the above can see in the input layer cells presented in the table 1. That if the target day is called $Q(t)$ the input layer of this group of simulations are the five that $Q(t-2)$, $Q(t-3)$, $Q(t-4)$, $Q(t-5)$, $Q(t-6)$.

On the other hand the second group of the simulations are composed of $Q(t-1)$, $Q(t-2)$, $Q(t-3)$, $Q(t-4)$, $Q(t-5)$ as the input layer data. The spread parameter was taken 0.53 and the number of neurons were taken as 10. 148 days data was trained and then tested for the real time data of next 7 days.

The output layer cell was called as $Q(t)$ was forecasted with a mean square error (MSE) of 15.16 with an R^2 of 0.913. Here R^2 refers as the determination coefficient that is commonly known as the square of correlation coefficient.

Figure 11 and Figure 12 represents the results of the third group simulations according to input layer cells.

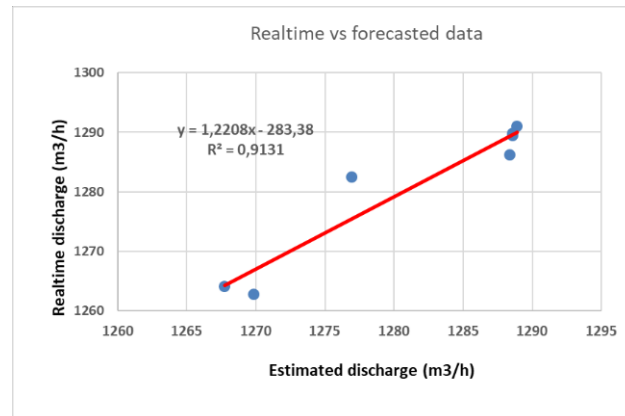


Figure 11. Correlation of Observed data and forecasted data in the third group simulations.

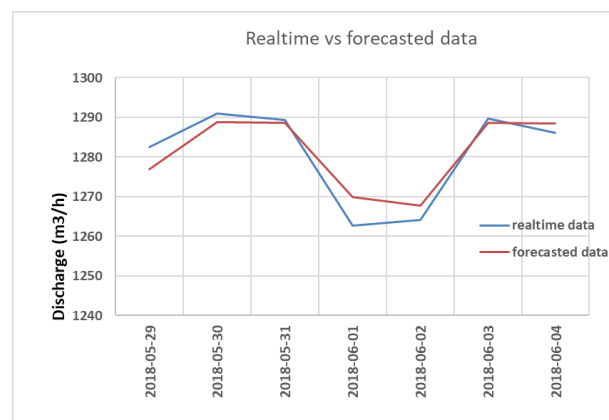


Figure 12. Observed data and forecasted data in the third group simulations.

4. CONCLUSIONS

One of the most common neural network methods, the radial basis functions are employed for forecasting the future value of production well discharges in a geothermal power plant. In neural network simulations of this paper the estimations were based on the previous daily measurements and daily statistical parameters such as mean and standard deviation. It was shown that neural networks methods provide satisfactory estimations reflected in performance evaluation criteria and in plots. The output tables of the study gives us the idea that the number and type of input layer elements are very important. Another important outcome is that the types of the parameters in the input layer affects the resulting forecast very sensitively.

Table 1: Summary of RBF simulations

Input layer cells	Spread parameter	Output layer cell	Number of training Data	Number of test data	Mean square error	R ²
Q(t-1), Q(t-2), Q(t-3), Q(t-4), Q(t-5), Q(t-6),	0.53	Q(t)	148	7	14,06	0.9909
Q(t-1), Q(t-2), Q(t-3), Q(t-4), Q(t-5),	0.54	Q(t)	148	7	19,89	0.9875
Q(t-2), Q(t-3), Q(t-4), Q(t-5), Q(t-6)	0.53	Q(t)	148	7	15,16	0.9131

REFERENCES

- Bilgin, O. (2018), The Importance of Geothermal Energy Resources in Turkey. Open Access Library, Journal, 5: e4317. <https://doi.org/10.4236/oalib.1104317>
- Demirbas, A. (2002) Turkey's Geothermal Energy Potential. *Energy Sources* , 24, 1107-1115. <https://doi.org/10.1080/00908310290087030>
- J.M.K.C. Donev et al. (2017). Energy Education- Geothermal power plants (Online). Available: https://energyeducation.ca/encyclopedia/Geothermal_power_plants. (accessed: March 1, 2019)
- Ajith A., Ninan S. and Babu J., (2001) Will We Have a Wet Summer? Long-term Rain Forecasting Using Soft Computing Models, Modelling and Simulation, Publication of the Society for Computer Simulation International, Prague, Czech Republic, Kerckho@s E.J.H. & Snorek M. (Eds.), ISBN 1565552253, pp. 1044-1048, 2001.
- Broomhead, D. and Lowe, D., (1988). "Multivariable functional interpolation and adaptive networks", *Complex Syst.* 2: 321–355.
- Poggio, T. and Girosi, F., (1990). "Regularization algorithms for learning that are equivalent to multilayer networks". *Science* 2247: 978–982.